PHYSICAL REVIEW B VOLUME 19, NUMBER 2 15 JANUARY 1979

# Optical properties of the radical cation tetrathiafulvalenium ($TTF^+$) in its mixed-valence and monovalence halide salts

J. B. Torrance,* B. A. Scott, B. Welber, F. B. Kaufman, and P. E. Seiden
*IBM Research Center, Yorktown Heights, New York 10598*
(Received 7 August 1978)

Measurements are presented of the optical properties of the radical cation $TTF^+$ (tetrathiafulvalenium) in a variety of different conditions: as $TTF^+$ monomers in solution, as $(TTF^+)_2$ dimers in solution, in the monovalence $(TTF)Br_{1.0}$ solid, and in the mixed-valence $(TTF)Br_{0.79}$ salt. From a comparison of these spectra and from polarized measurements on single crystals, the observed absorption peaks are unambiguously assigned as either intramolecular (excitons) or intermolecular (charge-transfer bands). It is shown that the organic metal $(TTF)Br_{0.79}$ has two such charge-transfer bands, at 0.6 and 1.5 eV. The existence of the lower-energy band is related to the high conductivity of this salt, and both of these are shown to be due to the mixed-valence nature of this salt. From the oscillator strength (plasma frequency) of this band, we infer a bandwidth along the stacks of $4t \sim 1.1$ eV, the largest yet reported for an organic metal. From the energy of the higher-frequency charge-transfer band, we infer that the effective Coulomb correlation energy is $U \sim 1¼$ eV, comparable with other organic salts. Nevertheless, the larger bandwidth in $(TTF)Br_{0.79}$ causes the Coulomb correlations to be relatively less important than in TCNQ (tetracyano-*p*-quinodimethane) salts, for example. A comparison is also made of the corresponding spectra for $TCNQ^-$, $TMTTF^+$ (tetramethyl-$TTF^+$), and $TSeF^+$ (tetraselenafulvalenium, the selenium analogue of $TTF^+$).

## I. INTRODUCTION

Interest in the $\pi$-molecular donor TTF (tetrathiafulvalene) originated with the discovery by Wudl and co-workers[1] that chlorine oxidation of this compound resulted in a salt with high electrical conductivity. Further study of these materials[2-5] has revealed and demonstrated the importance of a number of concepts and principles which are fundamental to these salts as well as to the more extensively studied salt[6] TTF-TCNQ (TCNQ, tetracyano-*p*-quinodimethane). A considerable amount of experimental work has been reported on the TTF salts formed with the simple halides[1-3,5,7-20] (Cl, Br, and I) and pseudo-halides[15,16,21-23] (SCN and SeCN). In some of these materials, the dc conductivity at room temperature is observed to be $\sim 400\ \Omega^{-1}\text{cm}^{-1}$, which is nearly as high as that of TTF-TCNQ. The fact that this high conductivity in the TTF halides is occurring on only one kind of "one-dimensional" stack (the TTF stack) makes these systems potentially simpler to understand than the two-stack conductors, such as TTF-TCNQ and NMP-TCNQ (NMP, N-methylphenazyl). In addition, the degree of oxidation (or average valence), $\rho$ of the TTF molecules in $(TTF)\text{-}Br_\rho$, for example, can be directly determined from the Br composition,[24] whereas its determination is more subtle[6] in TTF-TCNQ. Indeed, a comparative study[2,3,5] of the two salts $(TTF)\text{-}Br_{0.79}$ (metallic) and $(TTF)\text{-}Br_{1.0}$ (insulating) dramatically reveals the importance[25-28] of mixed valence in the entire class of conducting organic solids. The structure and composition of these TTF-halide salts also give solid evidence regarding the nature of ionic bonding in organic charge-transfer salts[4,5] and its important role in determining the average valence, $\rho$ (degree of oxidation).[4,5,26]

In this paper we present[3] an experimental study of the optical properties of TTF and some of its halide salts, which compliments the very recent work of Sugano, Yakushi, and Kuroda.[18] The optical properties of monovalence ($\rho = 1$) stacks of organic radical molecules are straightforward and relatively well understood, both experimentally and theoretically. The case of a mixed-valence ($\rho < 1$) stack, on the other hand, is much more complex and not fully understood. There has been some experimental work reported on mixed-valence TCNQ salts, but the results and interpretations are not unambiguous (Sec. V). As in the case of other electronic properties, the TTF-halide systems have a number of important advantages for studying optical properties: (i) there is only one optically active stack (i.e., the one composed of TTF molecules). (ii) The molecules are oriented in these structures[2,3,9,13,16,23] with an eclipsed overlap and hence the molecular and stacking axes are orthogonal. (The important consequence of this type of overlap is that the charge-transfer excitations along the stacks are not mixed or coupled to the intramolecular excitations, which are polarized in the plane of the molecule. This mixing is a serious complication in TCNQ salts which have slipped overlap.) (iii) The spectra of salts with different valence can be compared, such as $(TTF)\text{-}Br_{0.79}$ and

 

$(TTF)$-$Br_{1.0}$. (iv) The absorption peaks in the visible and ultraviolet turn out to be much better resolved than in the case of TCNQ salts. (v) Two bands, which are accidentally at the same energy for TCNQ, are nondegenerate for TTF (see text).

Before presenting the optical spectra of the solids, we first give in Sec. II the solution spectra of the molecules $TTF^0$ and $TTF^+$, which help establish the energies of the principal intramolecular excitations. A comparison with the spectrum of $(TTF^+)_2$ dimers in solution indicates the simplest effects of *inter*molecular interaction, including the presence of a charge-transfer band. In Sec. III the single-crystal and powder spectra of the monovalence $(TTF)$-$Br_{1.0}$ are given and compared with the solution spectra. Finally, both single-crystal reflectivity and powder absorption results on the mixed-valence salts [e.g., $(TTF)$-$Br_{0.79}$] are presented in Sec. IV. With the aid of the polarization measurements and comparison with the spectra presented earlier, an interpretation is given for the mixed-valence salts in terms of intra- and intermolecular transitions. In Sec. V, this interpretation is discussed with respect to previous interpretations of similar spectra for the $\pi$-electron acceptor TCNQ. In the conclusion, we focus on the quantitative analysis of the $(TTF)$-$Br_{0.79}$ spectrum and what can be learned about the relative magnitude of the tight-binding bandwidth $4t$ along the stacks and the effective intramolecular Coulomb repulsion energy $U$. It is concluded that $U/4t \sim 1$, significantly smaller than estimates[29] of ~2 for TCNQ salts. In the Appendix, we present the solid and solution spectra of the halide salts of TMTTF (tetramethyl-TTF) and TSeF (tetraselenafulvalene, the selenium analog of TTF).

## II. SOLUTION SPECTRA

Before examining the spectra of solids containing molecules of TTF, it is particularly helpful to examine the spectra of these molecules in solution, where they are (relatively) isolated and noninteracting. In Fig. 1 we show the solution spectra[30,31] of $TTF^0$ (long dashed lines) and $TTF^+$ (short dashed lines), obtained from ethanol solutions of TTF and $(TTF)$-$Cl_{1.0}$. Both spectra are in agreement with previous measurements.[32] For $TTF^+$, the energies of the absorption peaks are listed in Table I, together with similar data for $TMTTF^+$ and $TSeF^+$, discussed in the Appendix. For $TTF^+$, the weak absorption peak at 2.14 eV, the shoulder at 2.5 eV, and the peaks at 2.85 and 3.7 eV may be assigned[18] to the four lowest allowed transitions calculated[33] for $TTF^+$: $b_{2g} \rightarrow b_{1u}$,

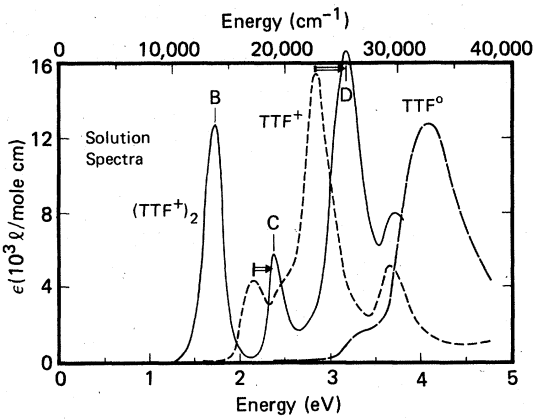


FIG. 1. Spectra of $TTF^0$ (— —) and $TTF^+$ (----) in acetonitrile solution at 300 °K, along with spectrum of $(TTF^+)_2$ dimers (——) in ethanol at 225 °K. Arrows represent Davydov shift of energy of monomer transitions upon dimerization. *B*, *C*, and *D* are the energies of the peaks in the dimer spectrum, and the units of absorption are discussed in Ref. 31.

$b_{1u} \rightarrow b_{3g}$, $b_{1u} \rightarrow b_{2g}$, and $b_{3g} \rightarrow b_{1u}$, each of which is predicted to be polarized in the plane of the $TTF^+$ molecule. Such intense low-energy absorption bands as in Fig. 1 are typical of the intramolecular spectra of conjugated $\pi$-molecular radicals.

As the solution of $TTF^+$ is cooled to lower temperatures, the spectrum is observed to change from the short-dashed line in Fig. 1 to the spectrum shown as the solid line. Such changes in the solution spectra upon cooling are commonly found for other ion radicals,[34-38] both anions and cations. From the temperature dependence of both the optical and EPR spectra in these other systems, it has been determined that this change is caused by the dimerization of the radical ions at low temperatures. From a comparison of the changes in these optical spectra[34-38] with those in Fig. 1, as discussed below, one can conclude that the low-temperature spectrum (solid line) is undoubtedly that of $(TTF^+)_2$ dimers. Focusing first on the principal features of the monomer spectrum, the weak absorption peak at 2.14 eV and the strong one at 2.85 eV, we see that they are each shifted (by ~0.3 eV or 2500 cm$^{-1}$) to higher energy upon dimerization. This shift is the usual Davydov shift,[39,40] which is expected due to the interaction between the transition dipole moments on adjacent molecules in the dimer. Since the transition dipoles are side-by-side

$+ \longleftarrow -$

$+ \longleftarrow -$

for an *intra*molecular transition of the planar mole-

TABLE I. Energies of the principal absorption peaks for the monomer and dimer in solution for $TTF^+$, $TMTTF^+$, and $TSeF^+$. See also Figs. 1, 11 and 12.

| | | *B* | *C* | *D* | *E* |
|---|---|---|---|---|---|
| $TTF^+$ | Dimer | 1.73 eV (14 000 $cm^{-1}$) | 2.39 eV (19 300 $cm^{-1}$) | 3.18 eV (25 600 $cm^{-1}$) | |
| | Monomer | ••• | 2.14 (17 200) | 2.85 (23 000) | 3.65 (29 400) |
| $TMTTF^+$ | Dimer | 1.60 (12 900) | 2.18 (17 500) | 3.03 (24 400) | |
| | Monomer | ••• | 1.91 (15 400) | 2.70 (21 700) | 3.82 (30 800) |
| $TSeF^+$ | Dimer | 1.60 (12 900) | 2.03 (16 400) | 2.83 (22 800) | 3.31 (26 700) |
| | Monomer | ••• | 1.77 (14 300) | 2.82 (22 700) | 3.10 (25 000) |

cules of a dimer, the dipole interaction is repulsive. Thus, there is an extra energy required to excite this transition, and hence its energy is "blue-shifted" (increased) with respect to the monomer. (In other cases, the transition dipoles moments may be oriented head to tail

$$+\leftarrow - \quad +\leftarrow -$$

giving rise to a Davydov red shift). The observed magnitude of this shift is comparable with those found for other ion radical dimers.[34-38]

In addition to these two intramolecular excitations, labeled C and D for the dimer in Fig. 1, there is a new low-frequency absorption peak labeled B at 1.73 eV (14 000 $cm^{-1}$) in the dimer spectrum, not present in that of the monomer. By analogy with other solution dimer systems,[34-38] this new absorption is assigned as a charge-transfer band, i.e., an *inter*molecular excitation not possible in a monomer, as shown schematically in Fig. 2. (This proposed assignment is verified by the polarized single-crystal measurements discussed in Sec. III.) The energy of this charge-transfer band is given by[41]

$$h\nu_{CT} = \tfrac{1}{2}[U + (U^2 + 16t^2)^{1/2}]$$
$$\approx U + 4t^2/U, \quad (4t)^2 \ll U^2. \tag{1}$$

In this expression, $t$ is the electron transfer integral between molecules and $U$ is the effective Coulomb interaction which is given by $U = U_0 - V_1$, where $U_0$ is the intramolecular Coulomb repulsion energy between two electrons on the same TTF molecule (or, equivalently, the disproportionation energy of $TTF^+ + TTF^+ \rightarrow TTF^{2+} + TTF^0$) and $V_1$ is the Coulomb repulsion energy between two electrons on adjacent molecules. Using Eq. (1) and an estimate of $4t \sim 1.1$ eV (obtained in Sec. VI) and $h\nu_{CT} = 1.73$ eV, we find $U = 1.5$ eV as an estimate of the effective Coulomb correlation energy $U$.

From the spectra in Fig. 1 we then conclude that there are two *intra*molecular excitations (labeled *C* and *D*) in this region, and the effect of the neighboring molecules in the dimer is to shift the energy of these excitations higher by ~0.3 eV. The existence of neighboring molecules also makes it possible to excite a new *inter*molecular transition or charge-transfer band (labeled *B* in Fig. 1), the energy of which measures the effective Coulomb interaction. Similar solution spectra have been obtained for TMTTF and TSeF and are included in the Appendix and in Table I.

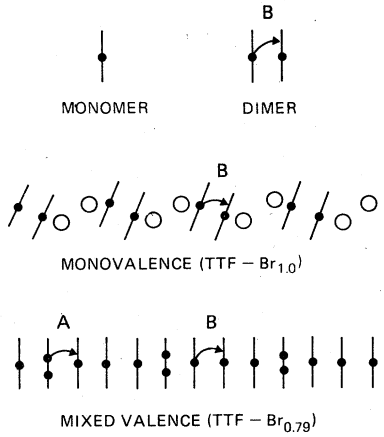


FIG. 2. Schematic diagram of the types of charge-transfer bands possible in a solution dimer, the monovalence salt $(TTF)Br_{1.0}$, and in the mixed-valence salt $(TTF)Br_{0.79}$. Note that • represents an unpaired electron on a TTF molecule (|) and ○ represents a bromide ion.

### III. MONOVALENCE (1:1) SALTS

In addition to the highly conducting mixed-valence phase of the TTF halides, Scott *et al.*[5] have discovered a phase with a 1:1 composition. These materials were prepared as discussed in detail in Ref. 5. The isomorphic structures of (TTF)-$Br_{1.0}$ and (TTF)-$Cl_{1.0}$ have been determined[5] and are shown in Fig. 3. The basic units in this unusual structure are $(TTF^+)_2$ dimers which alternate along the $c$ axis with pairs of nonbonded $Br^-$ ions. The overlap between the $TTF^+$ molecules within the dimers is eclipsed (directly overlapping), with a close interplanar spacing of 3.34 Å. The absorption spectrum of this solid of $(TTF^+)_2$ dimers might be expected to be very similar to the $(TTF^+)_2$ dimers in solution (Fig. 1) (assuming that the overlap in solution is similar to that in Fig. 3). Note that the molecular planes are not perpendicular to the $c$ axis, but are tilted so they make an angle of 66°. Thus the intramolecular excitations, which are polarized[33] in the molecular plane, will absorb weakly for light polarized along the $c$ axis: $\sim\cos^2 66°$, or about 17%. Therefore, the absorption of these transitions will be primarily (~83%) perpendicular to the $c$ axis. Similarly, the charge-transfer transitions, which are polarized along the line between the centers of two adjacent molecules, will be polarized primarily parallel to the $c$ axis.

Absorption measurements have been made on powdered samples, dispersed in KBr.[42] The powder absorption spectrum for (TTF)-$Cl_{1.0}$ is shown by the dashed line in Fig. 4, where it is compared with the spectrum of the solution $(TTF^+)_2$ dimer. Clearly, the spectrum of the solid composed of $(TTF^+)_2$ dimers is strikingly similar to that of $(TTF^+)_2$ dimers in solution. This dramatic similarity demonstrates the molecular nature of these solids and their optical properties. In addition, the reflectance spectrum of a small single crystal of (TTF)-$Br_{1.0}$ was measured at room temperature using a special optical microspectrophotometric system described elsewhere.[43] The reflectivity spectrum is shown in Fig. 5 for light polarized parallel and perpendicular to the $c$ axis. From these data, we can confirm the identification of the absorption peaks made in Sec. II: peak $C$ is an intramolecular excitation (polarized primarily perpendicular to the $c$ axis), while peak $B$ is a charge-transfer band (polarized primarily along the $c$ axis), as indicated schematically in Fig. 2.

The reflectivity data in Fig. 5 could, in principle, be analyzed more quantitatively by fitting them to an assumed model (as we shall do for (TTF)-$Br_{0.79}$ in Sec. IV). Such fits confirm the polarization of the excitations $B$ and $C$ inferred from visual inspection of Fig. 5 and give values for the energies of the transitions which agree with those from the powder measurements (Fig. 4). Because of the narrow energy range over which we have data, however, these fits are not unique and hence the other fitting parameters do not have significant meaning.

Note that the energy of peak $C$ (2.2 eV) in the solid is somewhat lower than that (2.4 eV) of the

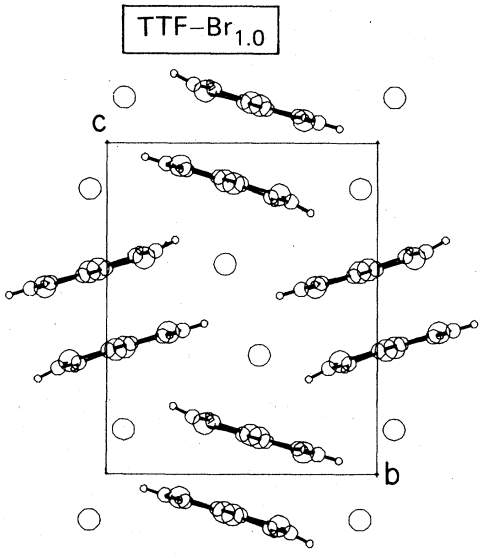


FIG. 3. Crystal structure of (TTF)-$Br_{1.0}$ and (TTF)$Cl_{1.0}$, as determined by Scott *et al.* (Ref. 5). Note that the $TTF^+$ molecules form dimers with an eclipsed overlap and a close interplanar spacing of 3.34 Å.

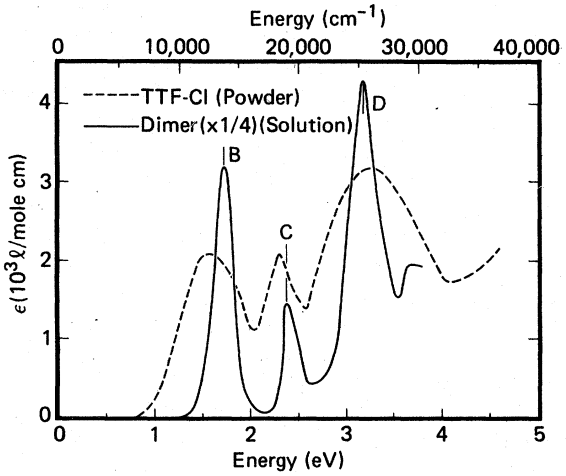


FIG. 4. Powder absorption spectrum of (TTF)$Cl_{1.0}$ (dashed line) compared with that of the $(TTF^+)_2$ dimer in solution. See Ref. 31.

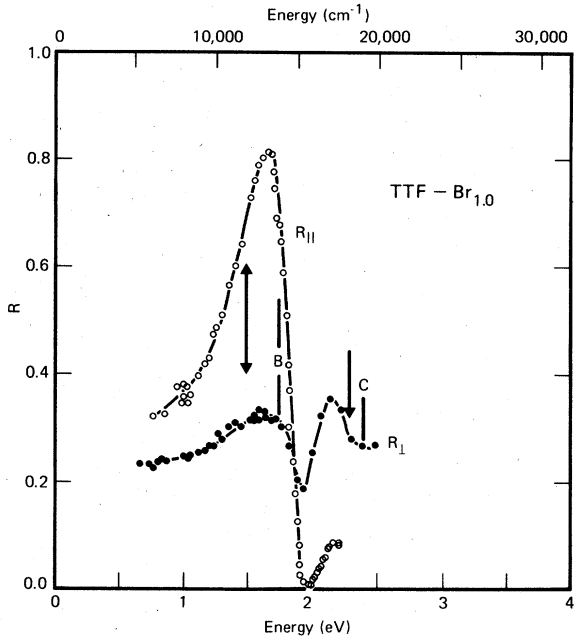


FIG. 5. Reflectance for light polarized parallel and perpendicular to the $c$ axis of a single crystal of (TTF)$Br_{1.0}$. For reference, the energies labeled $B$ and $C$ are those of the solution dimer and the arrows are the peak energies from the powder data in Fig. 4. The lines are hand drawn through the data.

dimer in solution. The energy of peak $B$ (1.5 eV parallel to $c$ and 1.7 eV perpendicular to $c$) is also somewhat lower than the 1.7-eV energy of the dimer charge-transfer band. These shifts and particularly the difference in energy found for radiation polarized parallel and perpendicular to the $c$ axis may be caused by Davydov shifts or some other effect in the solid. For the purpose of this paper, we shall regard these ~0.2-eV differences as an indication of the magnitude of the solid state or polarization effects and hence the order of magnitude of the errors which we should attach, for example, to our estimation of the parameter $U$. In the solid (TTF)-$Br_{1.0}$, $U$ is almost the same as for the $(TTF^+)_2$ dimers in solution (~1.5 eV).

Sugano, Yakushi, and Kuroda[18] have reported a monovalence (TTF)-$ClO_4$ salt, although the structure is as yet unknown. They reported the optical-absorption spectrum for a single crystal. The spectrum is very similar to the one (Fig. 4) we have found for the monovalence (TTF)-$Cl_{1.0}$ and the interpretation they have given is essentially identical with ours.[3] Similar spectra and interpretations have also been given for a variety of other monovalence organic salts, including salts of chloranil,[44] TMPD(tetramethyl-$p$-phenylenediamine),[45] TCNQ,[25,46-49] etc.

## IV. MIXED-VALENCE SALTS

The $c$ axis projected structure[2,5] of the mixed-valence salt (TTF)-$Br_{0.79}$ is shown in Fig. 6(a) and the (schematic) view down the $b$ axis in Fig. 6(b). As in the analogous structure[8,9,13] of (TTF)-$Cl_{0.80}$ and (TTF)-$I_{0.71}$, the TTF molecules and halide ions form separate stacks along the $c$ axis. The TTF molecules are stacked with an interplanar spacing of 3.57 Å, while in the structure shown in Fig. 6, the $Br^-$ ions are spaced uniformly at 4.54 Å. The unusual stoichiometry of these materials is directly related to the ratio of these lattice constants, i.e., $\rho = 3.57/4.54 = 0.79$. It has been shown[4,5] that the stoichiometry and hence the average valence $\rho$ of TTF in these ionic materials are determined by a competition between the electrostatic Madelung binding energy and the molecular energy $(I-A)$ of charge transfer, i.e., the ionization potential $I$ of TTF less the electron affinity $A$ gained by the halide. Differences in $A$ for Cl, Br, and I are the cause[4,5] of the variations in $\rho$ observed[5,24] for their mixed-valence TTF salts ($\rho \sim 0.80$, 0.79, and 0.71 for the Cl, Br, and I salts, respectively). For the purpose of this paper, the two most important points concerning the structure (Fig. 6) are: (i) that the

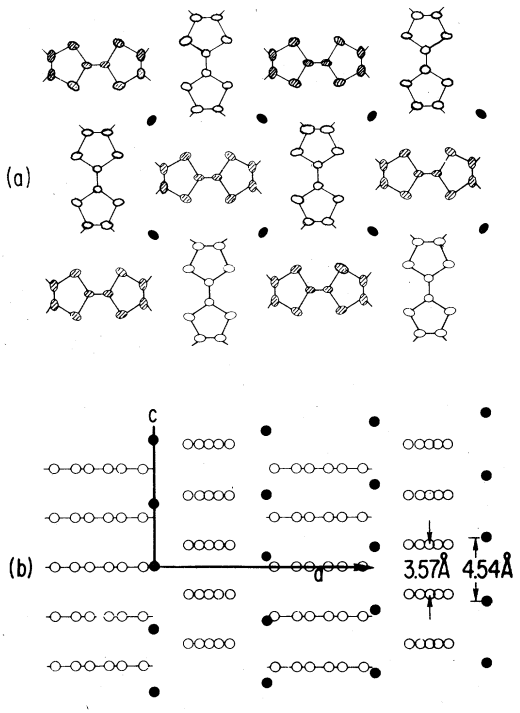


FIG. 6. Crystal structure of (TTF)$Br_{0.79}$ as viewed (a) down the $c$ axis (after Ref. 2) and (b) down the $b$ axis (schematic).

TTF stack is electronically mixed valence (as indicated by the stoichiometry) with an average valence $TTF^{+\rho}$, and (ii) that the overlap of neighboring TTF molecules along the stack is eclipsed, so that the molecular planes are perpendicular to the stacks and hence the *intra*-molecular excitations are not coupled or mixed with the charge-transfer excitations.

Single crystals and powder samples were prepared as described in detail in Ref. 5. The reflectance spectrum of a small single crystal of $(TTF)\text{-}Br_{0.79}$ was measured at room temperature. Both the reflectivity polarized parallel and perpendicular to the stacking axis are shown in Fig. 7. The absorption of a powdered sample dispersed in KBr is shown in Fig. 8 together with equivalent spectra for the mixed-valence chloride and iodide salts. It is clear from this figure that the spectrum of these salts is independent of the identity of the counter-ion (the halide), indicating that the absorption is caused by excitations in the TTF stacks. The dominant feature of the reflectivity data (Fig. 7) is the Drude-like edge near 1.2 eV (9700 $cm^{-1}$) observed for radiation polarized along the stack. This edge and the large value of the reflectivity at low frequency are related to the low-frequency absorption peak near 0.6 eV observed in the powdered samples, and both of these are related to the high dc conductivity of this salt: $\sigma \sim 400\ \Omega^{-1}cm^{-1}$ at 300 °K. In addition to this low-energy peak (labeled *A* in Fig. 8), the powder absorption spectrum shows three additional peaks, labeled *B*, *C*, and *D*, which are also found in the reflectance spectrum, as we shall see below.

A plasma edge has previously been reported in $(TTF)\text{-}I_{0.71}$ by Warmack and Callcott[14] and in $(TTF)\text{-}SeCN_{0.58}$ by Somoano *et al.*[22] and analyzed in terms of a simple Drude model. In our measurements (Figs. 7 and 8), we find an important additional peak near 1.5 eV (12 000 $cm^{-1}$), also present in our powder absorption data. Very recently, Sugano, Yakushi, and Kuroda[18] have reported single-crystal transmission measure-

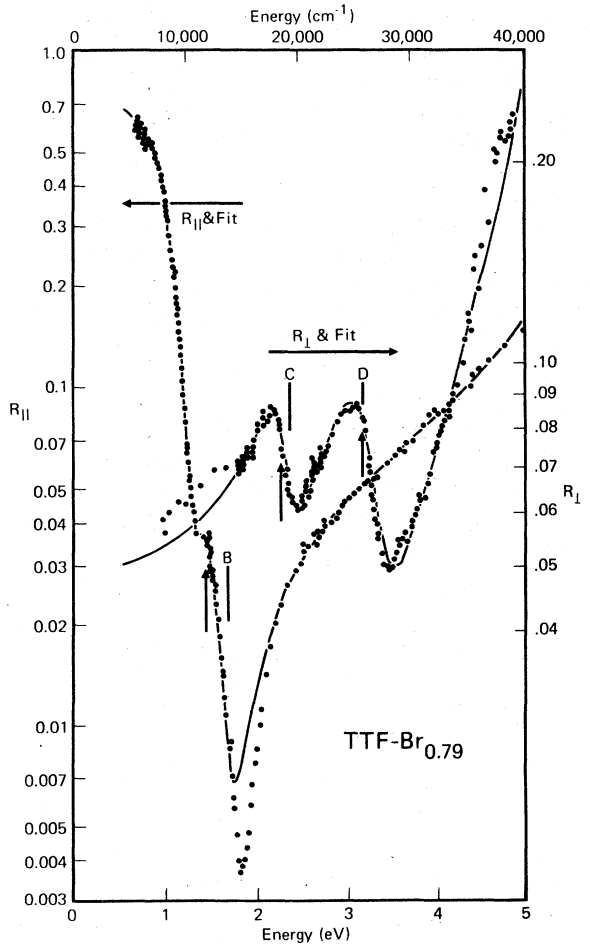


FIG. 7. Plot of the reflectance of a single crystal of $(TTF)Br_{0.79}$ for light polarized parallel and perpendicular to the stacking axis. The lines are a fit to the data using three Lorentz oscillators for each polarization, as discussed in the text. The parameters of the fit are given in Table II and the oscillator frequencies are indicated in the figure by the arrows. *B*, *C*, and *D* are the peak energies of the dimer, for comparison.

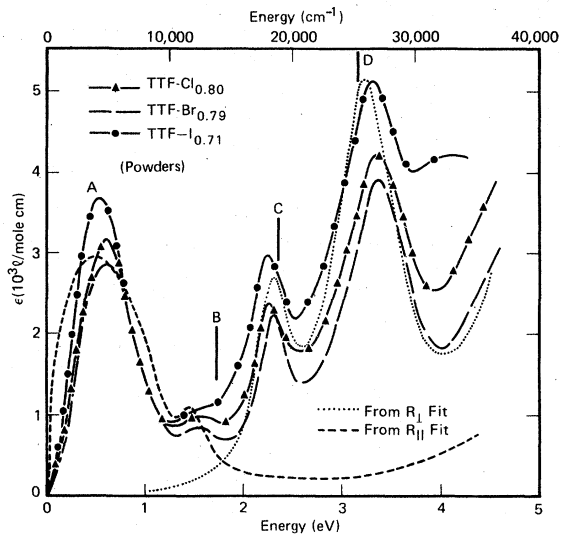


FIG. 8. Absorption spectrum of powdered samples of Cl, Br, and I salts of TTF, indicating that the major features are not associated with the halide. *B*, *C*, and *D* are the energies of the solution dimer, for reference. Also shown is the absorption predicted from the fit to the single-crystal reflectivity data (Table II) as discussed in the text and Ref. 51.

ments on (TTF)-$Br_{0.79}$, (TTF)-$I_{0.71}$, and (TTF)-$SCN_{0.53}$, in which they also observe the weak peak near 1.5 eV polarized along the stack. The other features and results of this excellent work are also in good agreement with ours.[3]

The reflectivity data of Fig. 7 can be analyzed more quantitatively if we assume that they are associated with a series of $N$ Lorentzian absorption peaks. This assumption appears quite reasonable, since the absorption (Fig. 8) appears to be caused by four such peaks. In this case, the dielectric function is given by

$$\epsilon(\omega) = \epsilon_\infty - \sum_i^N \frac{\omega_{pi}^2}{(\omega^2 - \omega_{0i}^2) + i\omega\Gamma_i}, \tag{2}$$

where $\epsilon_\infty$ is the magnitude of $\epsilon(\omega \to \infty)$, $\hbar\omega_{0i}$ is the energy of the $i$th absorption peak whose oscillator strength is described by a plasma frequency $\hbar\omega_{pi}$ and has a width given by $\hbar\Gamma_i$. For a series of such absorption peaks, the reflectivity is given by

$$R = \frac{1 + |\epsilon| - [2(|\epsilon| + \mathrm{Re}\epsilon)]^{1/2}}{1 + |\epsilon| + [2(|\epsilon| + \mathrm{Re}\epsilon)]^{1/2}}. \tag{3}$$

Thus we can use Eqs. (2) and (3) to fit the observed reflectivity and thereby represent the data by a series of Lorentz oscillators (absorption peaks).

Starting with the reflectivity for light polarized perpendicular to the stacking axis, the two bumps in the data in Fig. 7 near 2 and 3 eV suggest we try to use two Lorentz oscillators near these frequencies. The fact that the high-frequency reflectivity is not constant suggests that we will not be able to fit it with a constant $\epsilon_\infty$ alone. Thus we have fit the data with three Lorentz oscillators: one near 2 eV, one near 3 eV, and one at higher frequency to approximate the behavior of the dielectric constant in that region. But we emphasize that no particular physical significance should be ascribed to this third oscillator, the energy of which is outside the range of measurement. In order to reduce the number of parameters, we have set $\epsilon_\infty \equiv 1$. The results of such a least-squares fitting on Eqs. (2) and (3) to the perpendicular reflectance are shown by the solid line in Fig. 7 and the parameters of the three oscillators are listed in Table II.

Similarly for the case of the reflectivity polarized along the stack, the high value at low frequencies suggests a low-frequency oscillator, and the structure near 1.5 eV suggests a second one in that region. As in the other case, we represent the frequency dependence of $R$ at high frequencies by a Lorentz oscillator at an energy greater than 5 eV. In order to limit the number of parameters, we set $\epsilon_\infty = 1$ and set the frequency of the low-frequency oscillator to zero[50] (which corresponds to the Drude limit). The best fit is shown by the solid line in Fig. 7, using the parameters listed in Table II.

These reflectivity measurements (Fig. 7) can be compared to the powder absorption measurements (Fig. 8) by using the parameters in Table II and Eq. (2) to calculate the expected absorption.[51] The results are given in Fig. 8 for both parallel and perpendicular polarizations. The agreement is remarkable.

We should note that it is possible that peak $B$ in (TTF)-$Br_{0.79}$ might be a plasmon and not a charge-transfer band. Without any detailed predictions of the energy or polarization of such an excitation, it is not possible to rule out or con-

TABLE II. Values of parameters of three Lorentz oscillators used with Eq. (2) in best fit of reflectivity data of (TTF) $Br_{0.79}$ (Fig. 7), with $\epsilon_\infty \equiv 1$ fixed.

| Parameter | Oscillator 1 | 2 | 3 |
|---|---|---|---|
| $E\|\|$ STACK | | | |
| $\epsilon_\infty \equiv 1$ | | | |
| $\hbar\omega_0$ | $\equiv 0$ | 1.45 eV | 5.89 eV |
| (in units of $10^3$ cm$^{-1}$) | | (11.7) | |
| $\hbar\omega_p$ | 1.87 | 0.45 | 6.79 |
| $\hbar\Gamma$ | 0.29 | 0.34 | 0.41 |
| ($\tau$ in units of $10^{-15}$ sec) | (2.3) | (1.9) | |
| $E\perp$ STACK | | | |
| $\epsilon_\infty \equiv 1$ | | | |
| $\hbar\omega_0$ | 2.29 | 3.18 | 5.28 |
| (in units of $10^3$ cm$^{-1}$) | (18.4) | (25.6) | |
| $\hbar\omega_p$ | 0.88 | 1.63 | 5.43 |
| $\hbar\Gamma$ | 0.40 | 0.67 | 0.25 |
| ($\tau$ in units of $10^{-15}$ sec) | (1.65 | (0.98) | |

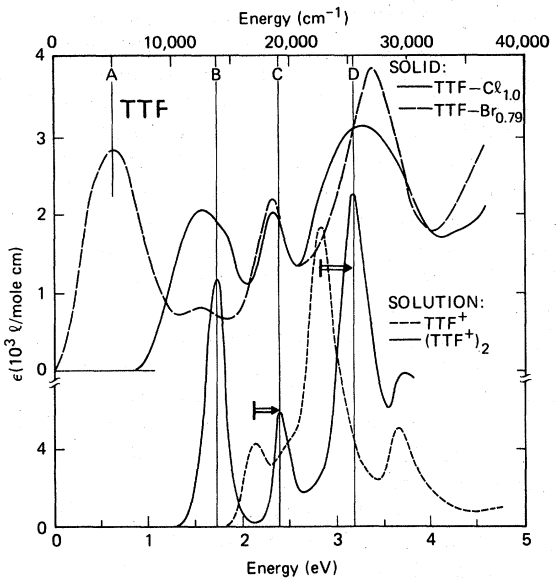


FIG. 9. Summary of the data from Figs. 1, 4, and 8, superimposed for comparison. From this figure, one can see the spectrum evolve from the monomer to the dimer to the monovalence salt to the organic metal (TTF)Br$_{0.79}$.

firm this possibility. Nevertheless, the comparison of the solution, monovalence and mixed-valence spectra described above, strongly suggests that this band is most likely due to a charge-transfer transition.

Thus the characteristic absorption spectrum of a mixed-valence stack of TTF molecules is quite simple. It consists of four distinct absorption peaks, labeled *A*, *B*, *C*, and *D* in Fig. 8. The two low-energy peaks *A* and *B* are charge-transfer bands, polarized along the stack,[52] while bands *C* and *D* are intramolecular, polarized within the molecular plane. Identical conclusions are reached by Sugano, Yakushi, and Kuroda[18] based on complimentary experiments. The interpretation of these bands, particularly the two charge-transfer bands, is discussed in the conclusion. The results of these sections are summarized in Fig. 9, where the absorption spectra are compared for the four cases discussed earlier.

## V. COMPARISON WITH TCNQ SPECTRA

As mentioned earlier, a large number of both anion and cation radicals exhibit[34–38] the same general behavior as found here for the cation radical TTF$^+$ in solution (Fig. 1). In addition, there are a number of examples of monovalence salts, the spectra of which are very closely related to that of the solution dimer, as we have found for TTF (Fig. 4): for example, K-chloranil,[44] tetramethyl-*p*-phenylenediamine (TMPD)ClO$_4$,[45] and K(TCNQ).[46–49] The interpretation which we have given in the case of (TTF)-Br$_{1.0}$ is generally the same as has been given earlier in these other cases. To our knowledge, however, there is only one other primary example of an organic system forming *mixed-valence* solids: salts of TCNQ. In this case, the interpretation of the spectra is not so clear.

The solution absorption spectra[35] of the TCNQ$^-$ monomer and (TCNQ$^-$)$_2$ dimer are shown in Fig. 10. For comparison, we also include the spectra[25] of the monovalence salt K(TCNQ) and the mixed-valence salt NMP-TCNQ. (The latter salt[53] is a mixed-valence system due to incomplete transfer of charge[25,26,54] from N-methylphenazyl to TCNQ.) A comparison of these TCNQ spectra with those for TTF (Fig. 9) reveals many strong similarities. The intramolecular excitations of the TCNQ monomer at 1.4 and 3.0 eV are Davydov shifted up in energy to 1.9 and 3.4 eV in the (TCNQ$^-$)$_2$ dimer and are labeled *C* and *D*. Polarized reflectivity measurements on K(TCNQ) clearly reveal that the peak at 1.1 eV is a charge-transfer band, somewhat lower in frequency (~0.3 eV) than that of the solution dimer (as in the TTF case). In the NMP-TCNQ spectrum, the low-frequency peak *A* is clearly the mixed-valence charge-transfer excitation, and is related to the high dc conductivity.

The identification of the band near 1.3 eV in NMP-TCNQ, however, is less clear. It has been assigned[25] to a charge-transfer band (type *B* in Fig. 2), analogous to the assignment in the

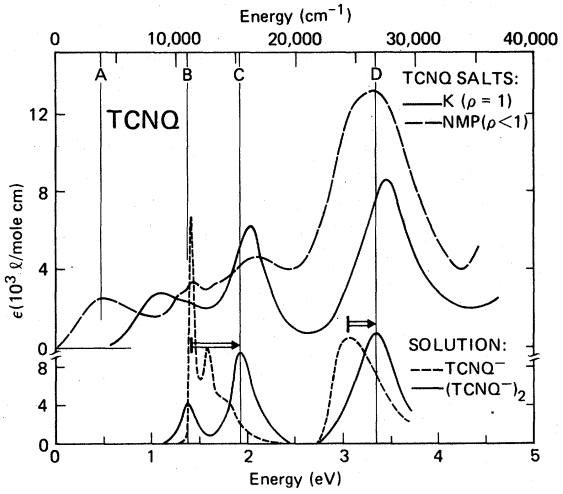


FIG. 10. For TCNQ$^-$, the spectra of the monomer and dimer in solution (Ref. 35), a monovalence salt [K(TCNQ)] and a mixed-valence salt (NMP-TCNQ) (after Ref. 25).

(TTF)-$Br_{0.79}$ case, but it has also been assigned[49,55,56] as an intramolecular excitation. There is some evidence to support each assignment,[57] but neither is conclusive. Part of the origin of this ambiguity is in the fact that the low-frequency transition in the TCNQ monomer (Fig. 10) has accidentally the same energy as the dimer charge-transfer band. [This is not the case for TTF (Fig. 1).] The fact that in these TCNQ salts the molecular plane is not perpendicular to the stacking axis gives rise to a strong[49] coupling and mixing between the intramolecular and charge-transfer excitations. This coupling makes it difficult to determine[57] the assignment from polarization measurements in the TCNQ salts. Thus while the interpretation of the spectra of the mixed-valence TCNQ salts remains inconclusive, the interpretation of the mixed-valence TTF salts is relatively clear.

## VI. CONCLUSION

In Fig. 9 the absorption spectra are compared for the mixed-valence and monovalence solids, as well as for the monomer and dimer of $TTF^+$ in solution. The most remarkable feature of these data is the striking similarity of the spectrum for the organic metal (TTF)-$Br_{0.79}$ with the spectrum of a pair of the $TTF^+$ molecules in solution. This comparison dramatically illustrates the molecular nature of these solids and the fact that the orbital energies and major electronic interactions of the molecules are only weakly altered when they are incorporated into a solid.

As discussed earlier, there are two intramolecular excitations of the $TTF^+$ molecule in this region of the spectrum (at 2.8 and 2.1 eV), the intensity of the high frequency one being several times as strong as the lower-frequency band. The effect of the presence of a neighboring $TTF^+$ molecule on these excitations is to Davydov shift them to higher frequencies (3.2 and 2.4 eV, respectively). This effect is observed to be almost the same for the $(TTF^+)_2$ dimers in solution and in the solid (TTF)-Cl, and even for the infinite stack of the (TTF)-$Br_{0.79}$ salt. Thus, the excitations labeled $C$ and $D$ in Fig. 9 are intramolecular excitations or molecular excitons.

Similarly, there is an absorption peak near 1.6 eV in the solution dimer and in both the monovalence and mixed-valence TTF halides, but not in the monomer spectrum. In the solution dimer and in the dimers of (TTF)-Cl, it is clear that this absorption is due to a charge-transfer transition. This is also the assignment as we have shown for the organic metal (TTF)-$Br_{0.79}$. The fact that the energy of this band, $h\nu_{CT}$, varies only slightly between these three quite different systems indicates the weak influence of crystal and solution environments on the effective Coulomb interaction $U$, which is $\sim 1\frac{1}{4}$ eV (at least at optical frequencies).

The strong similarity of the spectra of the $(TTF^+)_2$ dimers in solution and the dimers in (TTF)-Cl is not surprising. The important differences in the low-frequency spectra between insulating (TTF)-Cl and metallic (TTF)-$Br_{0.79}$ are clearly associated with the difference between monovalence and mixed valence in these salts. This difference gives rise to differences in the charge-transfer bands and are most readily discussed with the aid of Fig. 2. In the monovalence case, there is only one type of low-lying intermolecular excitation, labeled $B$ in Fig. 2, the energy of which is largely determined by the Coulomb repulsion between electrons. In a mixed-valence stack such a charge-transfer excitation is also possible where an electron is excited from a $TTF^+$ to a neighboring $TTF^+$ (Fig. 2). But in this case there is an additional, new type of charge-transfer excitation possible[25,46,47,49,54]: an electron from a $TTF^0$ molecule can be transferred to a neighboring $TTF^+$ (i.e., $TTF^0 + TTF^+ \rightarrow TTF^+ + TTF^0$). The energy of this new band is clearly much lower, since the large intramolecular Coulomb energies are not involved. It is this type of excitation, schematically described in Fig. 2, that is the origin of peak $A$ in mixed valence (TTF)-$Br_{0.79}$ and is called the mixed-valence charge-transfer band. An electron energy-band description can be used in order to describe these excitations more rigorously, in which case peak $B$ is described as an interband transition, while peak $A$ is an intraband transition.[25] As emphasized previously,[3,5,25,26] this new transition (peak $A$) is related to the dc conductivity and both this absorption peak and the high conductivity are due directly to the mixed-valence nature of the stacks.

It is of interest to understand how the oscillator strength of the electrons in a mixed-valence stack is distributed between the two types of charge-transfer bands: $A$ and $B$. In the monovalence case, peak $A$ is not possible and all of the intensity is in band $B$, as observed. In the mixed-valence case, there are no theoretical predictions as to the relative intensities of the two peaks. Experimentally, on the other hand, we can estimate the ratio of the observed oscillator strengths in peak $A$ and $B$ in (TTF)-$Br_{0.79}$ using the parameters in Table II:

$$(\hbar\omega_p^A)^2/(\hbar\omega_p^B)^2 = 17\,. \tag{4}$$

These considerations should be relevant to under-

standing the dc conductivity in different materials, in that a greater relative oscillator strength in the lower-frequency band ($A$) should result in higher conductivity. An equally important factor is the energy of peak $A$: in (TTF)-$Br_{0.79}$ $\sigma(\omega)$ peaks near 0.5 eV, compared with 0.1 eV for TTF-TCNQ.[58] Both of these factors merit further investigation.

An estimate of the electronic bandwidth of (TTF)-$Br_{0.79}$ can also be obtained from the oscillator strength (plasma frequency). For a simple one-dimensional tight-binding band (neglecting the unknown complications of Coulomb interactions)

$$4t = \rho(\hbar\omega_p)^2/4N_e e^2 c^2 \sin\pi\tfrac{1}{2}\rho\,, \tag{5}$$

$$= 17.4\rho(\hbar\omega_p)^2/N_e c^2 \sin\pi\tfrac{1}{2}\rho\,, \tag{6}$$

where $\rho$ is the degree of oxidation of the TTF stack. In Eq. (6) the plasma frequency ($\hbar\omega_p$) and the bandwidth ($4t$) are in units of eV, the $c$-axis lattice constant ($c$) is in Å, and the number of electrons contributing per volume ($N_e$) is in $cm^{-3}$. Using the value of $\hbar\omega_p^A = 1.87$ eV from Table II with Eq. (6), we obtain an estimate for the bandwidth:[59,60]

$$4t = 1.13 \text{ eV}. \tag{7}$$

Variations in the values of $\hbar\omega_p^A$ obtained from different fits to the data suggest an error of ±0.1 eV on the above estimate of the bandwidth. This value is the largest bandwidth yet reported for any organic conductor, but is not unexpected in view of the eclipsed overlap of the TTF molecules. In fact, recent calculations by Salahub, Messmer, and Herman[61] give a value of $4t \sim 1$ eV for the eclipsed overlap as in (TTF)-$Br_{0.79}$, but give a value 4–5 times smaller for the slipped geometry of TTF-TCNQ.

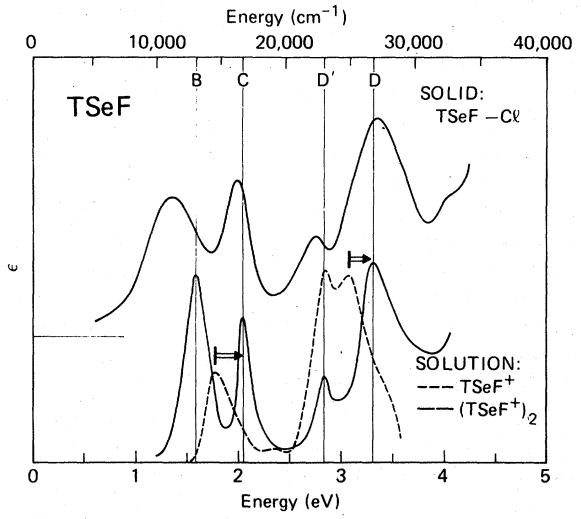


FIG. 12. Spectra analogous to Fig. 9 for TSeF.

From the energy of peak $B$, $\hbar\omega_0 = 1.45$ eV $= h\nu_{CT}$, we can use Eq. (1) with $4t = 1.1$ eV to obtain $U \sim 1.25$ eV. Therefore, we conclude that the Coulomb energies $U \sim 1\frac{1}{4}$ eV for the TTF-halide salts are comparable with those[25,29,56] in TCNQ salts, but the bandwidths in these systems are 2–5 times larger. Thus the relative role of Coulomb correlations will not be as strong in the TTF halides as in the TCNQ salts, consistent with the recent conclusions of Chaikin *et al.*[20]

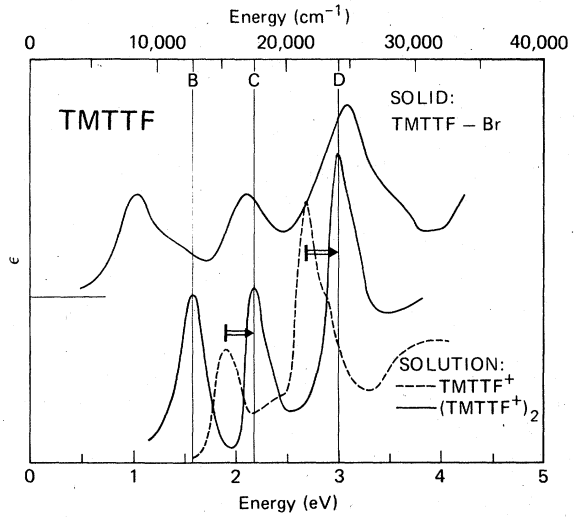


FIG. 11. Spectra analogous to Fig. 9 for TMTTF.

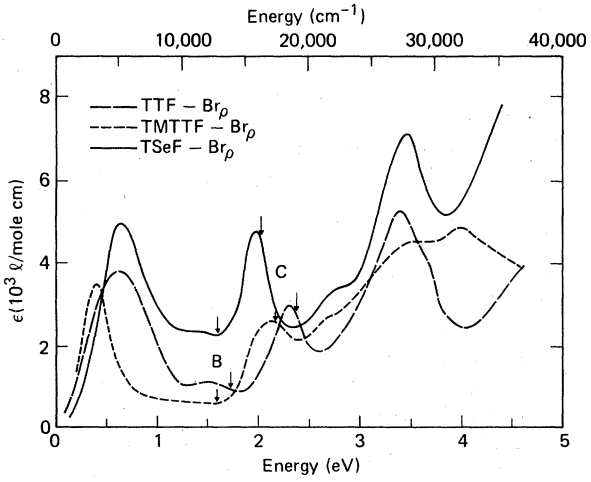


FIG. 13. Comparison of the spectra of the mixed-valence Br salts of TTF, TMTTF, and TSeF.

## ACKNOWLEDGMENTS

We wish to gratefully acknowledge the expert technical assistance of R. Linn and R. Thomas. We also thank P. M. Grant for advice and help in fitting the reflectivity data.


## APPENDIX: SOLID AND SOLUTION SPECTRA OF CLOSELY RELATED MOLECULES, TETRAMETHYL TTF$^+$ (TMTTF$^+$) AND TETRASELENAFULVALENIUM (TseF$^+$)

In this Appendix we include the spectra of some derivatives of TTF$^+$, namely, TMTTF$^+$ (tetramethyl-TTF$^+$) and TSeF$^+$ (the selenium analog of TTF$^+$). In Figs. 11 and 12 we show the solution spectra for both the monomer and dimer of these two molecules. The energies of these absorption peaks are included in Table I for comparison with the corresponding peaks for TTF$^+$. Also shown in Figs. 11 and 12 are the solid-state powder spectra for the monovalence salts, while the spectra of their mixed-valence salts are all compared in Fig. 13. As with the case of the TTF$^+$ spectra (Fig. 9), the interpretation of the spectra is most readily obtained by a careful comparison of the evolution of the spectra in going from the monomer to the solution dimer to the monovalence salt to the mixed-valence salt. Since this general behavior for TMTTF$^+$ and TSeF$^+$ is almost identical to that discussed earlier for TTF$^+$, our interpretation of Figs. 11–13 is directly analogous with that given for Fig. 9. In addition, the decrease in the energy of the low-frequency absorption peaks in going from TTF$^+$ to TMTTF$^+$ to TSeF$^+$ is the expected effect of methyl and selenium molecular substitution.

---

*Present Address: IBM Research Laboratory, San Jose, Calif. 95193


[1]F. Wudl, D. Wobschall, and E. J. Hufnagel, J. Am. Chem. Soc. 94, 670 (1972).

[2]S. J. LaPlaca, P. W. R. Corfield, R. Thomas, and B. A. Scott, Solid State Commun. 17, 635 (1975).

[3]The optical measurements reported here were first presented in: B. A. Scott, J. B. Torrance, S. J. LaPlaca, P. W. R. Corfield, D. C. Green, and S. Etemad, Bull. Am. Phys. Soc. 20, 496 (1975); J. B. Torrance, B. A. Scott, B. Welber, and F. B. Kaufman, *ibid.* 22, 424 (1977).

[4]J. B. Torrance and B. D. Silverman, Bull. Am. Phys. Soc. 20, 498 (1975); Phys. Rev. B 15, 788 (1977).

[5]B. A. Scott, S. J. LaPlaca, J. B. Torrance, B. D. Silverman, and B. Welber, J. Am. Chem. Soc. 99, 6631 (1977); Ann. N. Y. Acad. Sci. 313, 369 (1978).

[6]See, for example, *Chemistry and Physics of One-Dimensional Metals*, *NATO Advanced Study Institutes Series* (*B-Physics*), edited by H. J. Keller (Plenum, New York, 1977), Vol. 25.

[7]Y. Tomkiewicz, F. Mehran, D. C. Green, and B. A. Scott, Bull. Am. Phys. Soc. 19, 334 (1974).

[8]J. J. Daly and F. Sanz, Acta. Crystallogr. B 31, 620 (1975).

[9]D. J. Dahm, G. R. Johnson, F. L. May, M. G. Miles, and J. D. Wilson, Cryst. Struct. Commun. 4, 693 (1975).

[10]R. B. Somoano, A. Gupta, V. Hadek, T. Datta, M. Jones, R. Deck, and A. M. Hermann, J. Chem. Phys. 63, 4970 (1975).

[11]G. R. Johnson, D. J. Dahm, M. G. Miles, and J. D. Wilson, Bull. Am. Phys. Soc. 20, 466 (1975).

[12]R. J. Warmack, T. A. Callcott, and C. R. Watson, Phys. Rev. B 12, 3336 (1975).

[13]C. K. Johnson and C. R. Watson, J. Chem. Phys. 64, 2271 (1976).

[14]R. J. Warmack and T. A. Callcott, Phys. Rev. B 14, 3238 (1976).

[15]G. A. Thomas, F. Wudl, F. DiSalvo, W. M. Walsh, Jr., L. W. Rupp, and D. E. Schafer, Solid State Commun. 20, 1009 (1976).

[16]F. Wudl, D. E. Schafer, W. M. Walsh, Jr., L. W. Rupp, F. J. DiSalvo, J. V. Waszczak, M. L. Kaplan, and G. A. Thomas, J. Chem. Phys. 66, 377 (1977).

[17]T. Sugano and H. Kuroda, Chem. Phys. 47, 92 (1977).

[18]T. Sugano, K. Yakushi, and H. Kuroda, Bull. Chem. Soc. Jpn. 51, 1041 (1978).

[19]Y. Tomkiewicz and A. Taranko, Phys. Rev. B 18, 733 (1978).

[20]P. M. Chaikin, R. A. Craven, S. Etemad, S. J. LaPlaca, B. A. Scott, P. E. Seiden, Y. Tomkiewicz, J. B. Torrance, and B. Welber (unpublished).

[21]F. Wudl, J. Amer. Chem. Soc. 97, 1962 (1975).

[22]R. B. Somoano, A. Gupta, V. Hadek, M. Novotny, M. Jones, T. Datta, R. Deck, and A. M. Hermann, Phys. Rev. B 15, 595 (1977).

[23]H. Kobayashi and K. Kobayashi, Bull. Chem. Soc. Jpn. 50, 3127 (1977).

[24]The halide (or pseudohalide) composition inferred from chemical analysis is generally ~0.05 lower than the value inferred from x-ray measurements. We shall attempt to consistently use the latter values, except where only the former is known, as in (TTF)-$Cl_{0.80}$.

[25]J. B. Torrance, B. A. Scott, and F. B. Kaufman, Solid State Commun. 17, 1369 (1975).

[26]J. B. Torrance, Acc. Chem. Res. (to be published).

[27]J. B. Torrance, Ann. N. Y. Acad. Sci. 313, 210 (1978).

[28]J. B. Torrance, in *Molecular Metals*, *NATO Advanced Study Institute Series*, edited by W. E. Hatfield (Plenum, New York, to be published).

[29]J. B. Torrance, in Ref. 6, p. 137.

[30]Solutions were prepared in the following manner: absolute ethanol (100%) was degassed by bubbling $N_2$ gas into it for ~1h. Then, $10^{-3}$ M solutions of the chloride salt were made up and an initial spectrum was taken at 300°K. The solutions were then cooled to ~225 °K in an Oxford Instruments Dewar. These solu-

tions were stable and gave reversible spectral changes on cycling between the two temperatures.

[31]The absorption is expressed in the units of the molar extinction coefficient $\epsilon$(liter/mole cm) commonly used for solution spectra. $\epsilon$ is defined by: optical density $= \epsilon ct$, where $c$ is the concentration (moles/liter) and $t$ is the thickness (cm) of the sample. These units will also be used for our powder data and can readily be converted to the units appropriate for single-crystal solids $\alpha$ ($cm^{-1}$) by multiplying $\epsilon$ by 52 [for (TTF)-$Br_{0.79}$].

[32]S. Hünig, G. Kiesslich, H. Quast, and D. Scheutzow, Liebigs Ann. Chem. 310 (1973).

[33]R. Zabradnik, P. Carsby, S. Hünig, G. Kiesslich, and D. Scheutzow, Int. J. Sulfur Chem. C 6, 109 (1971).

[34]K. H. Hausser and J. N. Murrell, J. Chem. Phys. 27, 500 (1957).

[35]For TCNQ: R. H. Boyd and W. D. Phillips, J. Chem. Phys. 38, 2529 (1963).

[36]For chloranil (tetrachloro-*p*-benzoquinone): N. Sakai, I. Shirotani, and S. Minomura, Bull. Chem. Soc. Jpn. 44, 675 (1971).

[37]For TCNE (tetracyanoethylene): M. Itoh, Bull. Chem. Soc. Jpn. 45, 1947 (1972).

[38]For Würster's cations (methylated *p*-phenylenediamines): K. Kimura, H. Yamada, and H. Tsubomura, J. Chem. Phys. 48, 440 (1968).

[39]A. S. Davydov, *Theory of Molecular Excitons* (Plenum, New York, 1971).

[40]D. P. Craig and S. H. Walmsley, *Excitons in Molecular Crystals* (Benjamin, New York, 1968).

[41]P. Pincus, in *Selected Topics in Phys. Astrophysics and Biophysics*, edited by A. De Laredo and Jurisic (Reidel, Dordrecht-Holland, 1973), p. 138.

[42]A reliable and reproducible technique has been developed. The quality of the results is best seen in Fig. 8.

[43]B. Welber, Rev. Sci. Instrum. 47, 183 (1976).

[44]J. J. Andre and G. Weill, Chem. Phys. Lett. 9, 27 (1971), and Ref. 36.

[45]J. Tanaka and M. Mizuno, Bull. Chem. Soc. Jpn. 42, 1841 (1969); T. Sakata and S. Nagakura, Mol. Phys. 19, 321 (1970).

[46]Y. Iida, Bull. Chem. Soc. Jpn. 42, 71 (1969); ibid. 42, 637 (1969).

[47]S. Hiroma, H. Kuroda, and H. Akamatu, Bull. Chem. Soc. Jpn. 44, 9 (1971).

[48]S. K. Khanna, A. A. Bright, A. F. Garito, and A. J. Heeger, Phys. Rev. B 10, 2139 (1974).

[49]J. Tanaka, M. Tanaka, T. Kawai, T. Takabe, and O. Maki, Bull. Chem. Soc. Jpn. 49, 2358 (1976).

[50]For $\vec{E}$ parallel to stack, a somewhat better fit is obtained for a Lorentz oscillator at $\hbar\omega_0^A = 0.3$ eV, rather than the assumed Drude fit (with $\hbar\omega_0^A \equiv 0$). The former fit also better accounts for the peak at 0.6 eV seen in the powder absorption.

[51]Since light polarized along the $b$ (or $a$) axis in (TTF)$Br_{0.79}$ (Fig. 6) is perpendicular to the long molecular axes of half of the molecules, the extinction for $\vec{E} \perp \vec{c}$ must be doubled for calculating the expected powder absorption.

[52]From the deviation of the $E \perp c$ reflectivity data from the fit near 1.4 eV, one might suspect that some of peak $B$ is polarized parallel to $c$. Our analysis shows this to be a weak effect, but more convincingly, the single-crystal transmission data of Ref. 18 indicate that any absorption in this region for $\vec{E} \perp \vec{c}$ is $\lesssim 7$ times weaker than for $\vec{E} \parallel \vec{c}$.

[53]NMP-TCNQ was chosen because little or no absorption is expected from the cation stack: $NMP^+$ does not absorb below 3 eV and only small ($\sim 10\%$) concentrations of of $NMP^\circ$ are believed present.

[54]Z. G. Soos, Ann. Rev. Phys. Chem. 25, 121 (1974).

[55]P. M. Grant, R. L. Greene, and G. Castro, Bull. Am. Phys. Soc. 20, 496 (1975); and (unpublished).

[56]J. Hubbard, Phys. Rev. B 17, 494 (1978).

[57]J. B. Torrance, in *Organic Conductors and Semiconductors*, edited by L. Pal, G. Grüner, A. Janossy, and J. Solyom, *Lecture Notes in Physics* Series No. 65 (Springer-Verlag, Berlin, New York, 1977), p. 453.

[58]D. B. Tanner, C. S. Jacobsen, A. F. Garito, and A. J. Heeger, Phys. Rev. B 13, 3381 (1976).

[59]The fit in Ref. 14 to $(TTF)I_{0.7}$ near the plasma edge gave $\hbar\omega_p = 1.305$ eV, but correspond to a poor fit to data data over a very narrow energy range (0.7–1.8eV).

[60]The fit in Ref. 22 to the plasma edge in the (TTF-$SeCN_{0.58}$ gave $\hbar\omega_p = 1.78$ eV, in good agreement with our value of 1.87 eV. Their expression relating $\hbar\omega_p$ to $4t$, however, does not contain the necessary factor of $\rho$ in our Eq. (5).

[61]D. R. Salahub, R. P. Messmer, and F. Herman, Phys. Rev. B 13, 4252 (1976).